DTU Library

Noise Analysis of Switched-Current Circuits

Jørgensen, Ivan Harald Holger; Bogason, Gudmundur

Published in:
Circuits and Systems, 1998. ISCAS '98. Proceedings of the 1998 IEEE International Symposium on

Link to article, DOI:
10.1109/ISCAS.1998.704199

Publication date:
1998

Document Version
Publisher's PDF, also known as Version of record

NOISE ANALYSIS OF SWITCHED-CURRENT CIRCUITS

Ivan H. H. Jørgensen, Dept. of Information Technology, Technical University of Denmark, 2800 Lyngby, now OTICON A/S.

Gudmundur Bogason, OTICON A/S, Strandvejen 58, 2900 Hellerup, Denmark, Tel. (+45) 3917 7308, Fax. (+45) 3927 7000, E-mail: gb@icu.oticon.dk

ABSTRACT

The understanding of noise in analog sampled data systems is vital for the design of high resolution circuitry. In this paper a general description of sampled and held noise is presented. The noise calculations are verified by measurements on an analog delay line implemented using switched-current (SI) technique.

1. INTRODUCTION

In order to optimize circuits in the discrete time domain the noise properties must be known. The noise calculations of sampled data systems are complicated as the noise is sampled and held involving two or more clock phases. In section 2 the fundamental theory of sampled and held noise is presented.

In order to verify the noise calculations a test circuit was designed. This circuit is a switched current (SI) delay line consisting of 12 current copiers that delays the input for 6 clock cycles ($(z^{-1/2})^{12}$). This circuit and the measurements are presented in section 3 and these are compared with the theory developed in section 2. The noise calculation has finally been used to design a third order SI $\Sigma\Delta$-modulator[1], [2] and [3].

2. SAMPLED NOISE

In analog discrete time techniques such as switched capacitor and switched current the signals are sampled and held and thus the noise is also sampled and held. However, the bandwidth of the noise is normally larger than the sampling frequency and thus aliasing of the noise occurs. In the following the power spectral density (PSD) of sampled (actually undersampled) and held noise will be treated.

Assume that we have a bandlimited white noise source, $v_{nb}(t)$, that is sampled. The sampled bandlimited white noise, $v_{nb}^s(t)$, is expressed as:

$$v_{nb}^s(t) = v_{nb}(t) \cdot \delta_T(t) \tag{1}$$

where $\delta_T(t)$ is an infinite sequence of delta functions equally spaced in time with a sampling period T. From (1) the autocorrelation function for $v_{nb}^s(t)$ is easily found to be:

$$R_{nb}^s(t) = R_{nb}(t) \cdot f_s \delta_T(t) \tag{2}$$

where f_s is the sampling frequency. Consequently, the PSD, $S_{nb}^s(f)$, for the sampled bandlimited white noise is:

$$\begin{aligned} S_{nb}^s(f) &= S_{nb}(f) * f_s^2 \delta_{f_s}(f) && (3) \\ &= f_s^2 \sum_{n=-\infty}^{\infty} S_{nb}(f - nf_s) && (4) \end{aligned}$$

Now, the PSD, $S_{nb}(f)$, for the bandlimited white noise is assumed to be bandlimited by the transfer function $B(f)$, i.e., $S_{nb}(f) = S_n^w |B(f)|^2$ where S_n^w denotes the PSD for the white noise. Inserting this into (4) gives:

$$S_{nb}^s(f) = f_s^2 S_n^w \sum_{n=-\infty}^{\infty} |B(f - nf_s)|^2 \tag{5}$$

From [4] it is known that all of the noise power is folded down into the frequency band from 0 to f_s. In [5] it is shown that this leads to the fact that $\sum_{n=-\infty}^{\infty} |B(f - nf_s)|^2$ can be approximated by $\frac{BWN}{f_s}$ where BWN is the noise bandwidth. This approximation is valid as long as the cut-off frequency of the bandlimiting function $|B(f)|$ is equal to or higher than the sampling frequency [5]. This condition is normally fulfilled in order to ensure proper settling behavior in the analog circuitry. Assuming that the white noise is bandlimited by a first order system with a cutoff frequency of ω_0, the noise bandwidth is $BWN = \frac{\omega_0}{2}$ [5]. Therefore (5) can be written as:

$$S_{nb}^s(f) = f_s S_n^w \frac{\omega_0}{2} \tag{6}$$

Now, the noise is not only sampled but also held. Assuming that the sampled signal is held for a duration of τ then (6) becomes:

$$\begin{aligned} S_{nb}^s(f) &= \tau^2 \mathrm{sinc}^2(\pi f \tau) f_s S_n^w \frac{\omega_0}{2} && (7) \\ &= D^2 \mathrm{sinc}^2(\pi f \tau) \frac{S_n^w \frac{\omega_0}{2}}{f_s} && (8) \end{aligned}$$

where $D = \frac{\tau}{T}$ is the duty cycle.

Equation (8) describe the properties for the PSD of sampled and held white noise. In order to verify (8) a test circuit implemented in SI technique is designed.

3. A SI DELAY LINE

In order to verify (8) presented in the previous section a test circuit containing 12 cascaded current copiers (CCOPs) is designed. The circuit is shown in figure 1.

The output current can be taken from each CCOP, i.e., 12 output currents are available where the i'th output current is delayed ($-z^{-1/2}$) compared to the input current. The storage capacitances C_s is chosen so the power of the sampled and held noise in the CCOPs is quite large.

In order to calculated the noise from the SI delay line the term $S_n^w \frac{\omega_0}{2}$ in (8) must be determined. The $1/f$-noise in SI circuits are exposed to correlated double sampling (CDS), i.e., it is highpass filtered [5]. Hence, the noise in SI circuits is dominated by the white noise sources. Also, the noise current from the cascode transistors ($M_{2,i}$ and $M_{3,i}$ in figure 1) has no significant contribution to the overall noise current [5]. Thus, the noise current sources, in the CCOPs in figure 1, that contribute to the overall noise is the white noise sources from $M_{1,i}$ and $M_{4,i}$. Thus S_n^w in (8) for a single CCOP is:

$$S_n^w = \frac{2}{3} 2KT(g_{m1} + g_{mb1} + g_{m4} + g_{mb4}) \tag{9}$$

0-7803-4455-3/98/$10.00 © 1998 IEEE

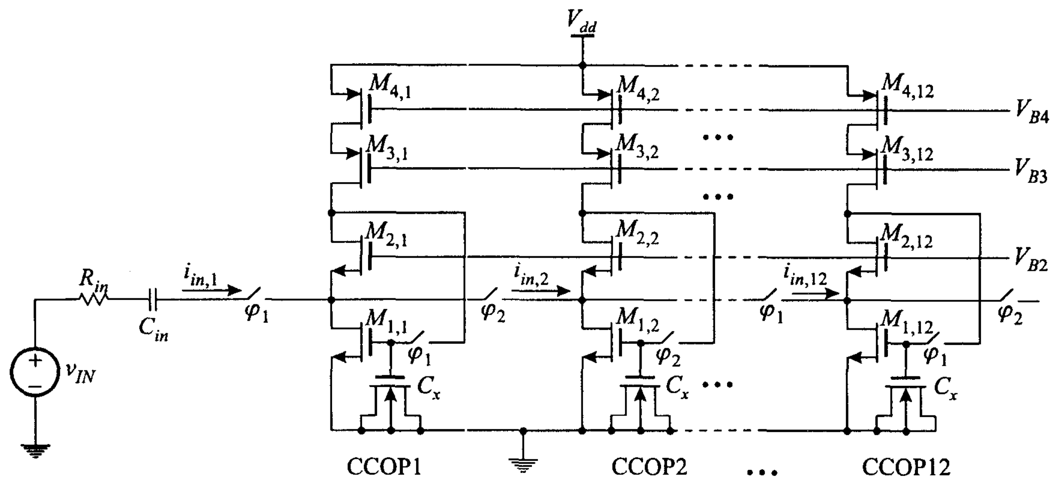

Figure 1. The SI delay line.

where g_{m1}, g_{m4}, g_{mb1}, and g_{mb4} is the transconductance and the transconductance to the bulk for $M_{1,i}$ and $M_{4,i}$, respectively. The bias voltages, V_{B2}, V_{B3} and V_{B4}, are generated on-chip by a bias circuit. The noise from the bias generator does not contribute the the PSD, S_n^w, because large decoupling capacitances are connected to the bias lines (V_{B2}, V_{B3} and V_{B4}) resulting in a cutoff frequency of approximately $1Hz$ for the noise sources in the bias generator.

The bandwidth of a the CCOPs is given by:

$$\omega_0 = \frac{g_{m1}}{C_s} \tag{10}$$

where C_s is the storage capacitance. From figure 1 the storage capacitance can be found as:

$$C_s = C_x + C_{gs1} + C_{gd2} + C_{bd2} + C_{gd3} + C_{bd3} \tag{11}$$

where the gate-source and the gate-drain capacitances also include their respective overlap capacitances.

Finally, it should be mentioned that for each CCOP in figure 1 the current is read out using a current mirror.

4. MEASUREMENT RESULTS

All of the measurements performed on the SI delay line are done using the FFT-analyzer HP3561A from Hewlett-Packard. The maximum frequency that can be measured, using this instrument, is $100kHz$. The output currents from the CCOPs are forced through a current-to-voltage converter constructed from a resistor and an Opamp. As the input resistance to the CCOP is extremely low (in the order of few ohms) a large external resistor, R_{in} (see, figure 1), is elegantly used to convert the external input voltage, v_{IN}, to a the input current, $I_{in,1}$.

Zero caused by sinc-function: The sinc-function in (8) causes the noise to be suppressed at certain frequencies. This occurs when $\text{sinc}(\pi f \tau) = 0$, i.e., $\pi f \tau = q\pi$. Therefore the frequencies where the sinc is zero is given by:

$$f = \frac{q}{\tau} = \frac{q}{DT} = \frac{q}{D} f_s \quad q = 1, 2, \ldots \tag{12}$$

This relation was verified by two series of measurements, one where the duty-cycle, D, was set to 0.25, 0.50 and 0.75 at a fixed sampling frequency of $10kHz$, and one where the sampling frequency was set to $5kHz$, $10kHz$ and $20kHz$ at a fixed duty-cycle of 0.50. The output current was taken from the last CCOP and the measured PSD is averaged 200 times. These measurements are shown in figure 2.

For a sampling frequency of $10kHz$ the zeros are located at:

$$f = \begin{cases} q \cdot 40.00kHz & , D = 0.25 \\ q \cdot 20.00kHz & , D = 0.50 \\ q \cdot 13.33kHz & , D = 0.75 \end{cases} \tag{13}$$

according to (12). These zeros are observed in figure 2 (a). Also, notice that the noise level at low frequencies changes as the duty-cycle is varied. This can be seen from (8) as the PSD is proportional to D^2. This will be studied in further details later.

Again, based on (12) the zeros will be located at:

$$f = \begin{cases} q \cdot 40kHz & , f_s = 20kHz \\ q \cdot 20kHz & , f_s = 10kHz \\ q \cdot 10kHz & , f_s = 5kHz \end{cases} \tag{14}$$

for a fixed duty cycle of $D = 0.50$. These zeros are observed in figure 2 (b). Further, notice that the noise level at low frequencies changes as the sampling frequency is varied. This can be seen from (8) as the PSD is inversely proportional to the sampling frequency. This, also, will be studied in further details later.

On each clock cycle some extra charge is stored on the storage capacitances due to charge injection and clock feedthrough phenomenons in the CCOPs. This can be seen in figure 2 as the large spikes located at $q \cdot f_s$.

Effect of duty-cycle: The power at the output of the CCOPs naturally drops to zero when the duty cycle approaches zero (only the continuous time noise from the output will be present). This can be seen from the first term in (8). To make the measurement more accurate this measurement was performed with a sinusoid at the input with a large amplitude. This can be done as the hold-function affects both the power of the noise and the sinusoid. The measurements are performed at a sampling frequency of $100kHz$ and with an input sinusoid with a frequency of $5kHz$. Since a large signal is used the measured PSDs are only averaged

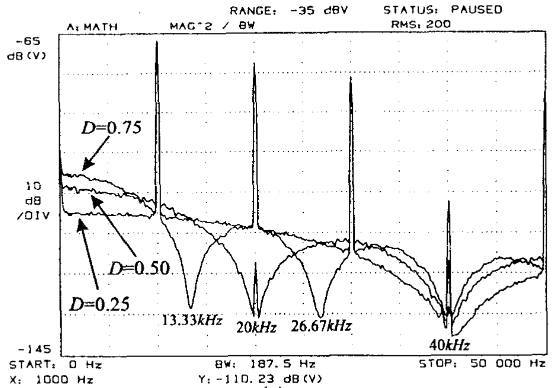

(a)

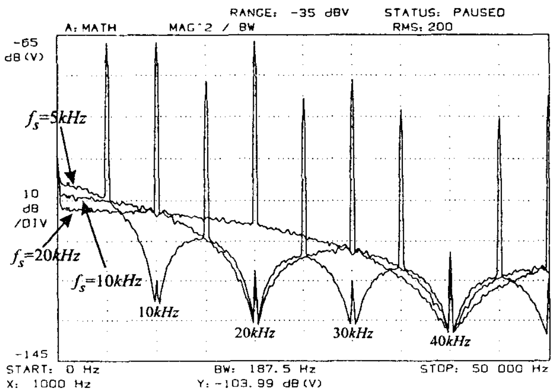

(b)

Figure 2. Noise shaping due to hold function. (a) fixed frequency. (b) fixed duty-cycle.

20 times. The output current was taken from the last CCOP. From (8) it can be seen that the PSD at the output must be proportional to D^2. In table 1 the PSD is shown as a function of the duty-cycle, also the normalized PSD is shown. The results clearly show that the PSD is proportional to D^2 as stated in (8).

Dependency on the sampling frequency: From (8) it can been seen that the PSD is inversely proportional to the sampling rate. To verify this, three measurements at different sampling rates were performed. During these measurements the PSD of the noise had to be measured. The measure PSDs, seen in table 2, are based on the average of 1000 FFT analysis in the frequency range $9kHz \le f \le 11kHz$. Again, the output current is taken from the last CCOP.

D	$(D/0.50)^2$	$S^s_{nb}(f)$ $[(nA)^2/Hz]$	Normalized
0.80	2.56	16420	2.561
0.70	1.96	12570	1.960
0.60	1.44	9236	1.440
0.50	1	6412	1
0.40	0.64	4083	0.637
0.30	0.36	2278	0.355

Table 1. Power spectral density as a function of duty-cycle. Last column is the normalized power spectral density: $\frac{S^s_{nb}(f)}{S^s_{nb}(f)|_{D=0.50}}$.

f_s $[kHz]$	$100kHz/f_s$	$S^s_{nb}(f)$ $[(pA)^2/Hz]$	Normalized
100	1	378.9	1
200	0.5	193.0	0.509
400	0.25	98.06	0.259
800	0.125	48.70	0.129

Table 2. Measured power spectral densities for different sampling rates. Last column is the normalized power spectral density: $\frac{S^s_{nb}(f)}{S^s_{nb}(f)|_{I=3.70\mu A}}$.

I $[\mu A]$	$I/3.70\ muA$	$S^s_{nb}(f)$ $[(pA)^2/Hz]$	Normalized
6.914	0.623	237.7	0.627
11.09	1	378.9	1
23.04	2.08	784.2	2.07

Table 3. Measured power spectral densities for different quiescent currents. Last column is the normalized power spectral density: $\frac{S^s_{nb}(f)}{S^s_{nb}(f)|_{f_s=100kHz}}$.

The sampling frequency used during these measurements is $100kHz$.

By comparing the expected and measured normalized values in table 2 it is clear that the PSD is inversely proportional to f_s.

Dependency on quiescent current: From (9) it can be seen that the PSD is proportional to $S^w_n \frac{\omega_0}{2}$. Since both S^w_n and ω_0 is proportional to g_{m1} the PSD must be proportional to the quiescent current, I, in the CCOPs as $g_{m1} \propto \sqrt{I}$. The PSD (averaged 1000 times) at the output of the last CCOP was measured for three different quiescent currents. The results are shown in table 3. The expected and the measured normalized PSD correspond very well.

Spectral density of sampled and held noise: The PSD of the sampled and held noise from a single CCOP cannot be measured directly as noise sources before the first CCOP will also be present. Furthermore, continuous time noise sources in the CCOP, that reads out the current, and continuous time noise sources on the PCB test board will also be measured. But as the SI delay line contains 12 cascaded CCOPs the PSD can be measured at the output of each and hence the PSD of the sampled and held noise for a single CCOP, $S^s_{nb}(f)$, can be determined.

First, the PSD at the output of each CCOP must be found. The output noise from the first CCOP must naturally be the PSD of the sampled and held noise plus same extra PSD called $S_a(f)$ containing all other noise sources. The second CCOP naturally samples the noise sources from itself. Also, the noise sources from CCOP1 will be sampled and finally the noise that was sampled and held by the first CCOP is stored in CCOP2. Thus, the total PSD at the output of CCOP2 must be $3S^s_{nb}(f) + S_a(f)$. Here it is assumed that the PSD $S_a(f)$ is the same no matter from which CCOP the output is taken. This is a fair assumption since all output section are designed identically and thus only the mismatch between these will cause $S_a(f)$ to differ from one output to another. The above argumentation can be continued and it can be seen that the PSD at the output of the i'th CCOP increase by $2S^s_{nb}(f)$ compared to the PSD at the output of the proceeding CCOP. The PSD at the output of the i'th

CCOP can thus be expressed as:

$$S_{o,i}(f) = (2i-1)S^s_{nb}(f) + S_a(f) \quad ,i = \{1, 2, \ldots, 12\} \quad (15)$$

where $S^s_{nb}(f)$ is the PSD given by (8). From the above equation it can be seen that the PSD at the output of the delay line increase linearly as a function of i. This can be used to distinguish the PSD of the sampled and held noise, $S^s_{nb}(f)$, from all other noise sources.

As the PSD of sampled noise is equally distributed between zero and the sampling frequency a low sampling frequency ($100kHz$) was used. In this way the PSD is quite high and the sinc-function does not affect the measurements at low frequencies. The PSD was measure at the output of all CCOPs in the delay line. The PSDs were measured in the frequency range between $9kHz$ and $11kHz$. The measured PSDs are averaged 1000 times to reduce the variance in the measurements. The result is shown in figure 3.

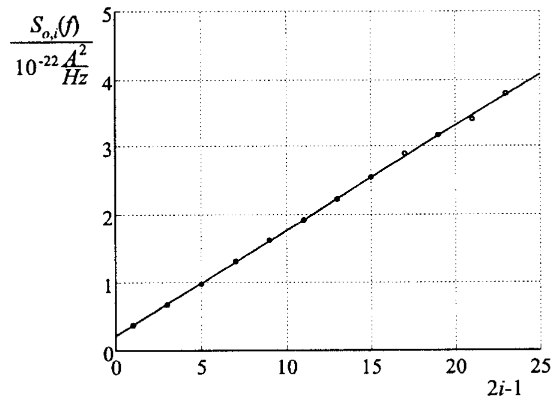

Figure 3. The measured power spectral density at the output. i is the number of cascaded CCOPs during the measurement.

From the 12 measurement points in figure 3, $S^s_{nb}(f)$ and $S_a(f)$ are found by approximating these with a 'best-fit'-line. This gives:

$$S^s_{nb}(f) = 15.46\frac{(pA)^2}{Hz} \quad (16)$$

$$S_a(f) = 21.96\frac{(pA)^2}{Hz} \quad (17)$$

This also shows that the PSD at the output depends linearly on the number of CCOPs used as stated in (15). Notice that $S_a(f)$ is larger than $S^s_{nb}(f)$. This clearly shows that it is necessary to use several measurement points to distinguish the sampled and held noise from all other noise sources. The measured PSD for the sampled and held noise can now be compared with the result found in (8). The quiescent current in the CCOPs during the measurements was $3.70\mu A$. A PSPICE simulation with the same quiescent current was performed. From this simulation the following parameters were found: $g_{m1} = 54.2\frac{\mu A}{V}$, $g_{mb1} = 8.70\frac{\mu A}{V}$, $g_{m4} = 26.6\frac{\mu A}{V}$, $g_{mb4} = 6.63\frac{\mu A}{V}$ and $C_s = 3.70pF$. Inserting the relevant parameter into (8), (9) and (10) the PSD is calculated to be:

$$S^s_{nb}(f) = 19.27\frac{(pA)^2}{Hz} \quad (18)$$

which only deviates by a factor of $\frac{19.27}{15.46} = 1.246$, which corresponds to 0.96dB, from the measured PSD.

In (8) it would probably be possible to measure ω_0 but it is not possible to measure S^w_n directly. Therefore it was chosen to compared the measured $S^s_{nb}(f)$ with simulations. Still, the measured and calculated PSDs correspond very well.

5. CONCLUSION

In this paper a noise analysis of analog sampled data systems is presented. A switched-current delay line has been designed to verify the noise calculations. A measurement technique is presented that makes it possible to distinguish the sampled and held noise from all other noise sources. Using this technique the PSD of the sampled and held noise of a single SI current copier is measured.

It is verified that the sampled and held noise is shaped by a sinc-function, that introduces zeros in the measured PSD that depend on the duty cycle and the sampling period. It is also verified that the PSD is proportional to the duty cycle squared and inversely proportional to the sampling frequency. Furthermore, it is shown that the PSD is proportional to the quiescent current in the switched current delay line. Finally, it is shown that the absolute level of the measured PSD correspond very well with the calculated level based values from simulations.

ACKNOWLEDGEMENTS

Ivan H. H. Jørgensen acknowledges the Ph.D. scholarship granted by the Danish Technical Research Council. Also, the authors would like to thank OTICON A/S for lending us the necessary measurement equipment.

REFERENCES

[1] Ivan H. H. Jørgensen and Gudmundur Bogason, "Design of a 3rd Order Micro Power Switched Current ΣΔ-Modulator", The third International Conference on Electronics, Circuits and Systems, ICECS'96, Rhodos, Greece. October 13-16, 1996, vol. 2 pp.948-951.

[2] Ivan H. H. Jørgensen and Gudmundur Bogason, "A 3rd Order Low Power Switched Current ΣΔ-Modulator", 14th Norchip conference, Norchip'96, Helsinki, Finland, November 4-5, 1996, pp.89-96.

[3] Ivan H. H. Jørgensen, "Current Mode Data Converters for Sensor Systems", Ph.D. Thesis, Dept. of Information Technology, Technical University of Denmark (DTU), April 1997.

[4] Jonathan H. Fisher, "Noise Sources and Calculation Technique for Switched Capacitor Filters", IEEE Journal of Solid-state Circuits, 1982, Vol. SC-17, pp. 742-752.

[5] Gudmundur Bogason, "Switched Current Circuits, Design, Optimization and Applications", Ph.D. Thesis, Electronics Institute, Technical University of Denmark (DTU), February 1996.